

Status of Lattice Flavor Physics

Matthew Wingate^a

^aInstitute for Nuclear Theory, University of Washington, Seattle, WA 98195-1550

This talk reviews recent lattice QCD calculations relevant for quark flavor physics. Since lattice results must be accurate and precise to play a definitive role in phenomenology, the focus is on unquenched results of quantities which can be calculated most reliably.

1. INTRODUCTION

In his talk which preceded mine, V. Lubicz did an excellent job summarizing the importance of lattice QCD results toward the goal of understanding quark flavor changing interactions, both within the CKM framework and beyond the Standard Model [1]. I. Shipsey gave a similarly inspirational talk describing the CLEO-c program, which will measure many quantities which are within reach of precise lattice predictions [2]. That comparison will generate confidence that lattice results for experimentally inaccessible quantities are correct. Those two talks provide ample motivation for this talk, in which I attempt to present a snapshot of the current efforts to contribute to the study of flavor physics. These are still the early days of unquenched lattice QCD. Unquenched simulations are being pushed deeper into the chiral regime, and systematic uncertainties are receiving increased scrutiny. Consequently, this talk should be read as a status report of ongoing research rather than a summary of completed work.

Accurate, precise results are required. Before one can claim to see new physics, the Standard Model result must be solid: uncertainties need to be controllable. The lattice QCD formulation provides an *ab initio* method for computing leptonic and semileptonic decay properties of hadrons. In practice, however, lattice simulations require at least one additional hypothesis. Because the light quark masses cannot be set to their physical values, data obtained with unphysically heavy quarks must be extrapolated to the physical limit. Chiral perturbation theory gives the

functional forms for these extrapolations, but this expansion cannot be applied if the quark masses are too large.

If one cannot firmly use chiral perturbation theory to extrapolate simulation results, then one is forced to extrapolate empirically, estimating the subsequent uncertainty by trying many fit functions. This introduces a hypothesis which is one step removed from the desired first principles QCD calculation. Current results based on simulations using Wilson-type fermions have used quark masses larger than $m_s/2$, which is on the border of the chiral regime. (Domain wall fermions simulations have been pushed to $m_s/4$.) It is hard to test these fitting ansätze without doing the lighter quark mass simulations. Of course the chiral regime will eventually be reached and, with it, greater theoretical control.

Staggered fermions are computationally inexpensive, so lighter quark masses can be used in simulations. Light sea quark masses as small as $m_s/10$ have been used to date. This allows one to simulate in a region of parameter space where chiral perturbation theory converges quickly. However, there is a price to be paid. An algorithmic trick is needed in order to have 3, not 4, active sea quark flavors. This “fourth-root” trick has not been theoretically justified, so one must hypothesize that staggered lattice QCD in the continuum limit is QCD. This hypothesis is testable, and has passed a first round. Fig. 1 shows results for several “golden,” or cleanly-computable, quantities divided by the experimentally determined value [3]. Calculations on the left-hand side were done in the quenched approximation, and those on the right-hand side used $2 + 1$ fla-

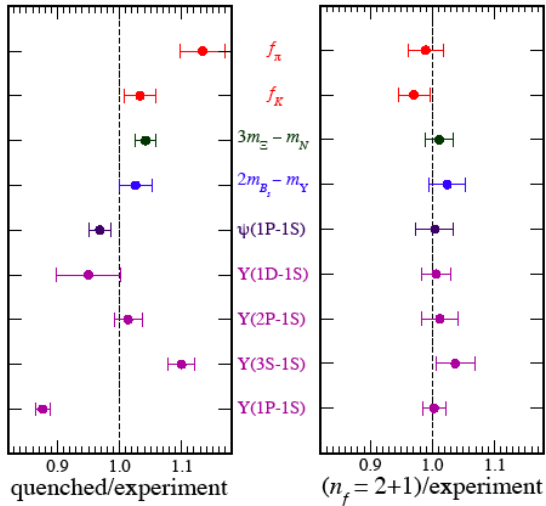


Figure 1. Comparison of quenched and unquenched results to experiment [3].

vors of dynamical staggered quarks (the MILC configurations, *e.g.* [4]).

I believe that these two hypotheses are complementary and both should be pursued until neither is necessary.

Due to time and space constraints, some choice had to be made about which topics to cover and which to omit. I have given priority to quantities most cleanly extracted from simulations and to results which include sea quark effects. I am unable to cover many interesting and important topics, most notably $K \rightarrow \pi\pi$ matrix elements (see *e.g.* [5]) and theoretical methods aimed at reducing systematic uncertainties in future calculations (see *e.g.* [6]).

2. DECAY CONSTANTS

The decay constant, f_M , for a meson M parameterizes the leptonic decay matrix element of the weak axial current:

$$\langle 0 | A_\mu | M(p) \rangle \equiv f_M p_\mu. \quad (1)$$

Matrix elements of this form are straightforward to compute in simulations. An additional renormalization calculation is needed to match the lat-

tice current(s) to the continuum current. The results presented below rely on perturbative calculations of the matching coefficients, and in some cases the uncertainty due to truncating the perturbative expansion is a leading source of uncertainty.

The B_s and D_s decay constants require no light quark mass extrapolation, so they are more straightforward to compute than f_B and f_D . These quantities have been computed using the 2+1 flavor MILC configurations. Using NRQCD for the b quark we found [7]

$$f_{B_s} = 260 \pm 7 \pm 28 \text{ MeV}. \quad (2)$$

In this work the statistical uncertainty is quoted first and the total systematic error second, unless noted otherwise. The systematic error in (2) is mostly due to assuming the truncated $O(\alpha_s^2)$ terms in the perturbative matching contribute with coefficient $O(1)$. A calculation of f_{B_s} on the same configurations using relativistic heavy quarks is underway by FNAL/MILC/HPQCD.

Several calculations of f_{B_s} have been done with $n_f = 2$. Although the strange sea quark is quenched, one argues that strange quark loop effects are small corrections. This may be true, but it takes us another step away from the *ab initio* calculation we desire. Results are summarized in Fig. 2. The only notable difference is between the JLQCD result [11] and (2). Before one attributes this to a difference between 2 and 3 flavor calculations in general, I think further investigation into the dependence on light sea quark mass is necessary. The lesson of Fig. 1 is that light sea quarks are needed for f_K , f_π , and Υ splittings, for example, to agree with experiment. JLQCD find that if the lattice spacing is set using f_K , then m_ρ and r_0 agree with experiment and phenomenology, respectively. However, it is also important that the Υ spectrum be reproduced. Comparing lattice spacings set with different quantities, CP-PACS [10] found $a_\rho/a_\Upsilon \approx 1.15$ on a coarse lattice and $a_\rho/a_\Upsilon \approx 1.20$ on a fine lattice. The JLQCD lattices are similar in quark mass and lattice spacing, so I speculate that one would find similar results for a_ρ/a_Υ (and thus for a_{f_K}/a_Υ) on the JLQCD lattices. If I include an uncertainty due to lattice spacing ambiguity in the same manner

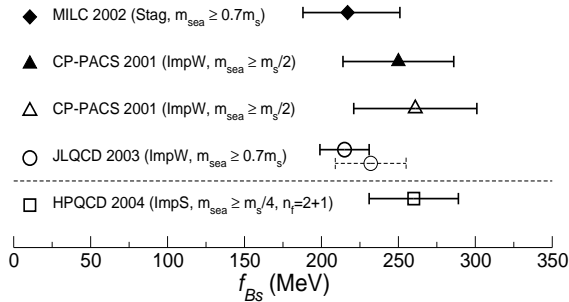


Figure 2. Summary of unquenched calculations of f_{B_s} (bold points) [8–11,7]. Solid points used the Fermilab heavy quark formulation and open points used NRQCD. All points above the dashed line have $n_f = 2$. The sea quark action and masses are noted in parentheses. The dashed point below the JLQCD result is discussed in the text.

as [10], then I obtain the dashed point in Fig. 2. Therefore, I conclude that difference between 2 and 2+1 flavor results for f_{B_s} cannot be resolved yet. On the other hand, there is no advantage to averaging them together, so I quote the 2+1 flavor result as the best current estimate.

Lattice NRQCD breaks down as the heavy quark mass is lowered to near the inverse lattice spacing. Consequently extrapolations must be performed to the charm sector, incurring a large systematic uncertainty. It is preferable to simulate directly at the charm quark mass using relativistic fermions. This can be accomplished on very fine lattices, treating the charm quark just like the strange and light quarks, or on lattices with any reasonable spacing using the Fermilab formulation [12]. A preliminary calculation of f_{D_s} on the MILC lattices using the latter method was presented here [13]. Fig. 3 shows $f_{D_s}\sqrt{m_{D_s}}$ as a function of sea quark mass. They find

$$f_{D_s} = 263 \begin{matrix} +5 \\ -9 \end{matrix} \pm 24 \text{ MeV}. \quad (3)$$

The quoted systematic uncertainty is mostly due to higher order in the heavy quark expansion. This calculation computes part of the matching nonperturbatively [14]; the remaining 1-loop cor-

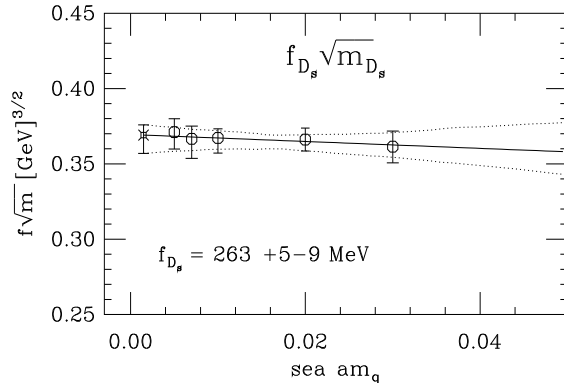


Figure 3. Unquenched calculation ($n_f = 2 + 1$) of $f_{D_s}\sqrt{m_{D_s}}$ vs. sea quark mass [13]. (The bare strange quark mass is 0.04 in lattice units.)

rection is small, so the quoted $O(\alpha_s^2)$ uncertainty is negligible at this level.

The D decay constant has also been computed in [13]. Computations were done at many points in the partially quenched parameter space, allowing a global fit to PQ χ PT including finite lattice spacing effects [15]. Fig. 4 shows $f_D\sqrt{m_D}/(f_{D_s}\sqrt{m_{D_s}})$ along the fully unquenched line of partially quenched parameter space; other plots with m_{sea} held fixed were shown too [13]. The extrapolated result obtained is

$$\frac{f_{D_s}\sqrt{m_{D_s}}}{f_D\sqrt{m_D}} = 1.20 \pm 0.06 \pm 0.06. \quad (4)$$

The error due to truncating the heavy quark expansion cancels in the ratio, so the leading systematic uncertainty is from the chiral fits. Combining (3) and (4), they find

$$f_D = 224 \begin{matrix} +10 \\ -14 \end{matrix} \pm 21 \text{ MeV} \quad (5)$$

where the dominant systematic uncertainty is from the heavy quark expansion.

Work by the FNAL/MILC collaboration on the B decay constant using relativistic fermions is underway. Since presenting some NRQCD results last year [16], our efforts have been devoted to improving the signal-to-noise ratio for f_B . Impressive improvement was seen by using smeared

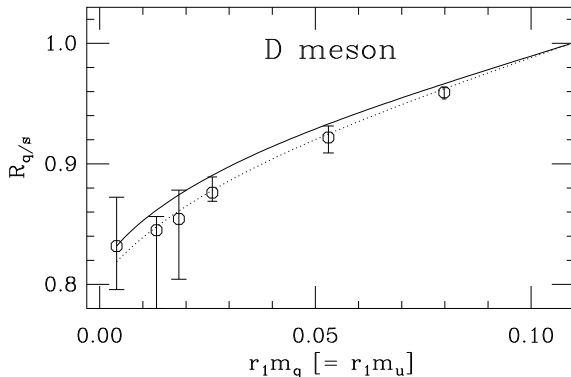


Figure 4. Unquenched calculation ($n_f = 2 + 1$) of $f_D \sqrt{m_D} / (f_{D_s} \sqrt{m_{D_s}})$ [13]. The global fit (dotted curve) to the data points, and to partially quenched data (not shown), includes taste-breaking $O(a^2)$ effects. The solid curve is obtained by subtracting these effects and yields the result in the text.

sources and sinks for the heavy quark [17]. Fig. 5 shows the ratio $\xi \equiv f_{B_s} \sqrt{m_{B_s}} / (f_B \sqrt{m_B})$ plotted vs. valence light quark mass. Current efforts will now be directed toward obtaining data at enough masses to permit a PQ χ PT fit as was presented for f_D . There are existing unquenched calculations which quote results for f_B based on extrapolations using $m_{\text{sea}} \geq m_s/2$ (e.g. [11]). However, due to the importance of this quantity for CKM constraints and to the possibility of previously unforeseen large curvature at small masses [18,19], I prefer to wait until the chiral extrapolation is under firmer control before quoting a result and uncertainty.

The simulations for heavy-light decay constants using the MILC lattices have been done using 1 lattice spacing and 1 volume so far. Finite lattice spacing errors have been estimated by assuming terms neglected in the low energy Symanzik effective theory appear with $O(1)$ coefficients. Simulations with finer lattices are underway to check this estimate. Finite volume effects were recently studied in heavy meson chiral perturbation theory [20] and estimated to be small compared to the other current uncertainties quoted above. However, they could contribute when chiral ex-

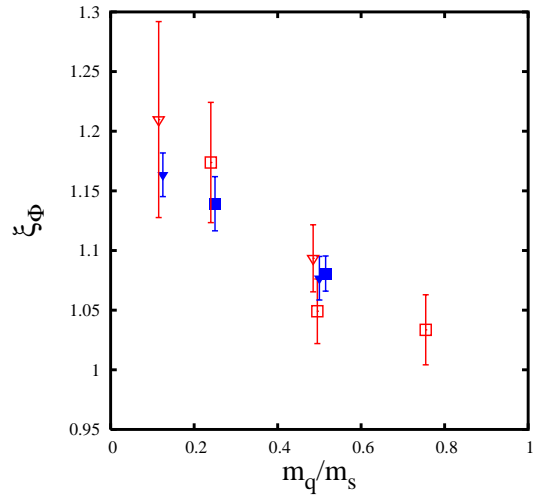


Figure 5. ξ vs. valence light quark mass in units of physical strange quark mass [17]. The open symbols used point sources and sinks while the solid symbols utilized smearing for the heavy quark propagator. Different symbols correspond to different sea quark masses.

trapolations of ξ are further along.

The predictions from heavy meson chiral perturbation theory are crucial ingredients for extrapolating lattice data to the physical light quark masses. At small quark masses, chiral logarithms become important. For example, in continuum heavy meson χ PT ξ has a term which goes like $(1 + 3g^2)m_\pi^2 \ln(m_\pi^2/\Lambda^2)$ times a known constant, where g is the $B - B^* - \pi$ coupling. Lattice data for this ratio will not be able to precisely computed g because simulations are done at masses where the logarithm is small. However, a large uncertainty for g will eventually contribute a significant error to ξ . Therefore, it is important to determine g directly. First results, in the quenched approximation, were published in [21] (for the charm sector) and [22] (for the bottom sector). It is important to repeat these calculations with 3 dynamical flavors, since only then are the low energy constants of chiral perturbation theory physical.

The f_π and f_K decay constants have been computed very precisely on the MILC configurations [23,24]. As pointed out in [25], their result for the ratio

$$f_K/f_\pi = 1.210 \pm 0.004 \pm 0.013 \quad (6)$$

can be combined with experimental measurements of the decay rates for π and K to $\mu\bar{\nu}_\mu$ to yield

$$|V_{us}| = 0.2219 \pm 0.0026 \quad (7)$$

where the error is dominated by lattice uncertainties. This result is in agreement with, and has the same uncertainty as, the 2004 PDG average $|V_{us}| = 0.2200 \pm 0.0026$ obtained from semileptonic K decay [26].

3. NEUTRAL B MIXING

Measurements of the mass and width differences in neutral B and B_s mixing can give us insight into flavor changing physics. Accurate computations of hadronic matrix elements of the relevant 4-quark operators are necessary ingredients in order to extract the high energy parameters. In the Standard Model, one needs to compute

$$\langle \overline{B^0} | (\bar{b}d)_{V-A} (\bar{b}d)_{V-A} | B^0 \rangle \equiv \frac{8}{3} f_B^2 m_B^2 B_B \quad (8)$$

to obtain $|V_{td}|$ from Δm_d . Note that the matrix element is parameterized by the factor B_B in a normalization such that $B_B = 1$ in the vacuum saturation approximation. The corresponding calculation for the strange B_s^0 , combined with the experimental lower bound for Δm_s , yields and even tighter constraint on $|V_{td}|$.

JLQCD results [11] are still the state-of-the-art. They quote, in the $\overline{\text{MS}}$ scheme at $\mu = m_b$

$$B_B = 0.836(27)_{\text{stat}} \begin{pmatrix} +0 \\ -27 \end{pmatrix}_\chi (56)_{\text{EFT}} \quad (9)$$

$$B_{B_s} = 0.850(22)_{\text{stat}} \begin{pmatrix} +18 \\ -0 \end{pmatrix}_\chi (57)_{\text{EFT}} \begin{pmatrix} +5 \\ -0 \end{pmatrix}_{m_s} \quad (10)$$

One expects the B factors to be less sensitive to chiral logarithms since their coefficient is much smaller than for the decay constant. Nevertheless a calculation using light staggered sea quark masses with $n_f = 2 + 1$ is underway [17].

The B_s width difference is dominated by loop diagrams with a charm quark, so a measurement of $\Delta\Gamma_{B_s}$ would determine $|V_{cb}^* V_{cs}|^2$. For this calculation another matrix element is needed in addition to B_{B_s} , the scalar bag factor:

$$\langle \overline{B_s^0} | (\bar{b}s)_{S-P} (\bar{b}s)_{S-P} | B_s^0 \rangle \equiv -\frac{5f_{B_s}^2 m_{B_s}^4 B_{S_s}}{3(m_b + m_s)^2}. \quad (11)$$

The best result to date is $B_{S_s}(m_b) = 0.86(3)(7)$ from [18] with $n_f = 2$ improved Wilson quarks. This computation is being done on the MILC lattices, but the matching calculation needs to be completed.

Even for physics beyond the Standard Model, lattice calculations of hadronic matrix elements are needed to connect the experimental measurements to theoretical parameters. For example, the complete set of five 4-quark operators for $B^0 - \overline{B^0}$ mixing have been computed in the quenched approximation [27].

4. SEMILEPTONIC DECAYS

Below we discuss how lattice calculations of the form factors governing semileptonic pseudoscalar states can be used to compute CKM matrix elements. The form factors parameterize the relevant matrix element of the weak current; *e.g.* for $B \rightarrow \pi \ell \nu$,

$$\langle \pi | V_\mu | B \rangle \equiv f_0(q^2) \frac{m_B^2 - m_\pi^2}{q^2} q_\mu + f_+(q^2) \left(p_\pi + p_B - \frac{m_B^2 - m_\pi^2}{q^2} q \right)_\mu \quad (12)$$

where q is the momentum transferred to the lepton pair. This matrix element can be computed on the lattice for a range of q^2 ; one cannot presently go to small q^2 without introducing lattice artifacts as $|\mathbf{p}_\pi| \rightarrow 1/a$.

$$\frac{1}{|V_{ub}|^2} \frac{d\Gamma}{dq^2} = \frac{G_F^2}{24\pi^3} p_\pi^3 |f_+(q^2)|^2 \quad (13)$$

can be integrated over q^2 using lattice data for the right-hand side. Then the partial width, determined by experiment, can be inserted, yielding $|V_{ub}|$.

A preliminary result using NRQCD on MILC configurations (with $m_{\text{sea}} = m_s/4$) was presented

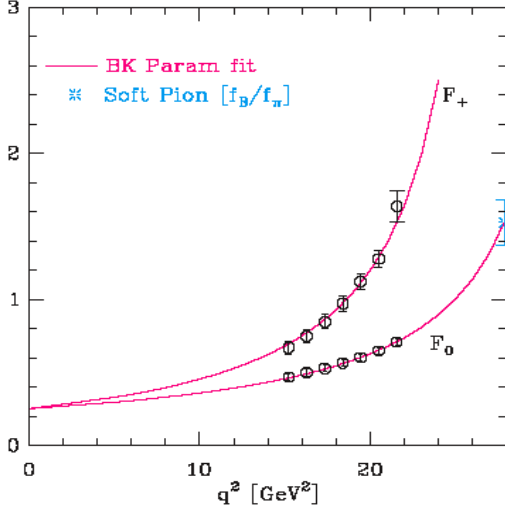


Figure 6. $B \rightarrow \pi \ell \nu$ form factors on the MILC configurations with NRQCD [28].

here [28]. Fig. 6 shows f_+ and f_0 vs. q^2 after chiral extrapolation of the valence quark mass. The data are well-fit by an ansatz which satisfies the kinematic constraint $f_+(0) = f_0(0)$; the heavy quark scaling laws $f_+(q_{\max}^2) \propto \sqrt{m_B}$, $f_0(q_{\max}^2) \propto 1/\sqrt{m_B}$ and $f_{+,0}(0) \propto m_B^{3/2}$; and includes the B^* pole and an effective second pole [29]. Integrating over the entire range of q^2 and taking branching ratios from CLEO [30] we obtain

$$|V_{ub}| = (3.86 \pm 0.32_{\text{expt}} \pm 0.58_{\text{latt}}) \times 10^{-3}. \quad (14)$$

CLEO has binned their data, so we can perform the integration over the restricted range $16 \text{ GeV}^2 \leq q^2 \leq q_{\max}^2$ to find

$$|V_{ub}| = (3.52 \pm 0.73_{\text{expt}} \pm 0.44_{\text{latt}}) \times 10^{-3}. \quad (15)$$

Note that this last step decreases the lattice uncertainty but more than doubles the experimental error. The moving NRQCD formulation [31,32] promises to permit simulations in an inertial frame moving with respect to the B , so that one can satisfy $|\mathbf{p}_\pi| \ll 1/a$ even with small q^2 .

Another preliminary result,

$$|V_{ub}| = (3.0 \pm 0.6_{\text{expt}} \pm 0.4_{\text{latt}}) \times 10^{-3}, \quad (16)$$

was reported here [33]. This is a fully unquenched calculation on the MILC lattices with the Fermi-

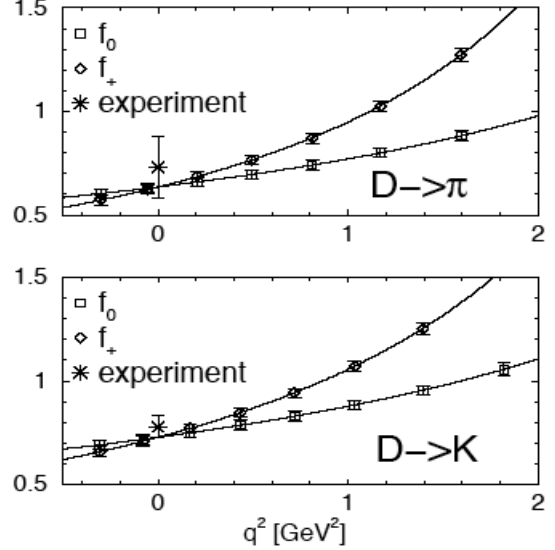


Figure 7. $D \rightarrow \pi \ell \nu$ and $D \rightarrow K \ell \nu$ form factors on the MILC configurations with the Fermilab formulation [34].

lab heavy quark formulation, where the integration uses the same restricted range of q^2 . One finds nice agreement between this result and the partially quenched NRQCD results above. As the authors of [28] and [33] extend their results on the set of MILC configurations, results will be highly correlated and a joint analysis would be the best way to extract a single result. At present the results (15) and (16) share configurations at only one value of $(m_{\text{val}}, m_{\text{sea}})$. For the purpose of quoting a single number here, I average the central values in (15) and (16), but just carry over the same experimental and lattice errors

$$|V_{ub}| = (3.3 \pm 0.7_{\text{expt}} \pm 0.4_{\text{latt}}) \times 10^{-3}. \quad (17)$$

The larger experimental error does not let us off the hook; extending the lattice results more accurately to lower q^2 will reduce both uncertainties, as (14) indicates.

Finalized results for the $D \rightarrow \pi \ell \nu$ and $D \rightarrow K \ell \nu$ form factors were presented here [33,34]. These used the Fermilab heavy quark formulation and fully unquenched light and strange quarks. The form factors and their q^2 dependence are

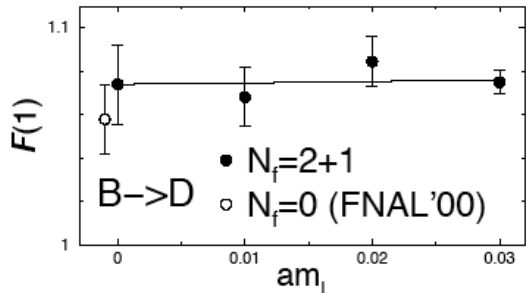


Figure 8. $B \rightarrow D l \nu$ form factor at zero recoil vs. sea quark mass (in lattice units; $am_s = 0.04$) [33].

shown in Fig. 7. Note the entire range of q^2 can be studied in the D rest frame without the pion having large spatial momentum in lattice units. Integrating the fits yields

$$|V_{cd}| = 0.239 (20)_{\text{expt}} (10)_{\text{stat}} (24)_{\text{sys}} \quad (18)$$

$$|V_{cs}| = 0.969 (24)_{\text{expt}} (39)_{\text{stat}} (94)_{\text{sys}}. \quad (19)$$

The leading lattice systematic uncertainty is due to the neglect of higher order terms in the heavy quark expansion.

Ref. [33] also presented a preliminary unquenched result for the $B \rightarrow D l \nu$ form factor evaluated at zero recoil, $\mathcal{F}_{B \rightarrow D}(w = 1) = 1.074(18)(16)$. Fig. 8 shows the light quark mass dependence of the form factor. Combining this result with experiment gives

$$|V_{cb}| = 0.038 \pm 0.006_{\text{expt}} \pm 0.001_{\text{latt}}. \quad (20)$$

The 3 results (18), (19), and (20) satisfy CKM unitarity:

$$(|V_{cd}|^2 + |V_{cs}|^2 + |V_{cb}|^2)^{1/2} = 1.00(2)(10) \quad (21)$$

where the first error is experimental and the second is from lattice. This is the first time such a test could be done using only inputs from experiment and unquenched lattice QCD.

Progress was made recently in calculating the $K \rightarrow \pi l \nu$ form factors [35]. Utilizing and extending the double ratio method developed for $B \rightarrow D l \nu$ decays [36], the form factors can be computed more precisely than before. A plot of

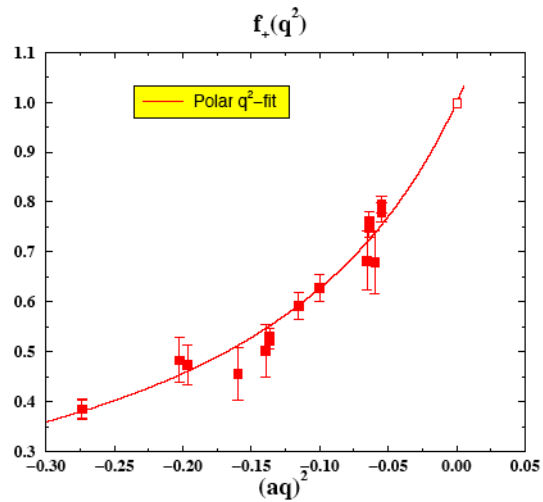


Figure 9. Quenched $K \rightarrow \pi l \nu$ form factor [35].

$f_+(q^2)$ in the quenched approximation is reproduced in Fig. 9. Using the value extrapolated to $q^2 = 0$ with experimental input yields

$$|V_{us}|^{\text{quenched}} = 0.2202 \pm 0.0025. \quad (22)$$

This precision is comparable to other methods, in particular (7), so it would be profitable to use this method in an unquenched calculation.

5. NEUTRAL K MIXING

In order for experimental measurements of $K^0 - \bar{K}^0$ mixing to constrain the CKM parameters $\bar{\rho}$ and $\bar{\eta}$, a precise determination in QCD of the matrix element

$$\langle \bar{K}^0 | O_{\Delta S=2} | K^0 \rangle \equiv \frac{8}{3} f_K^2 m_K^2 B_K \quad (23)$$

is necessary. There have been many quenched calculations of B_K ; a review was given recently in [37]. Several new results have appeared since that review [38–43].

The present situation of the quenched results, is murky, but perhaps not dire. Fig. 10 shows several different quenched results for B_K plotted vs. lattice K mass. The cross is a staggered fermion result in the continuum limit [44]. The rest of the

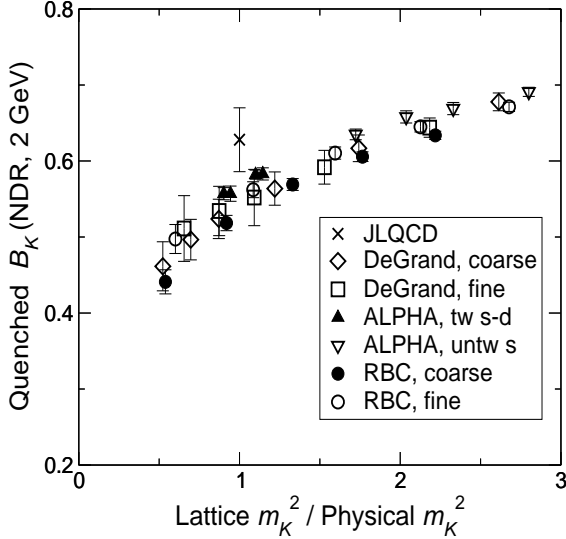


Figure 10. Quenched B_K as a function of m_K^2 . Selected results, in legend order: [44,45,39,40].

Table 1
Selected quenched B_K in the continuum limit (an asterisk indicates a 2 point extrapolation).

Ref.	fermions	$B_K(\overline{MS}, 2 \text{ GeV})$
[44]	staggered	0.628(42)
[46]*	DWF	0.575(20)
[39]	twisted m	0.592(16)
[40]*	DWF	0.570(20)

points are at a single lattice spacing, but are instructive nevertheless. One observes a downward curvature in B_K as one decreases the K mass, as expected from chiral perturbation theory. Reports of linear-only mass dependence have been made based on data which do not disagree with this plot: either the mass range covered is too narrow or m_K^2 is not small enough to resolve the curvature within statistical errors.

There is noticeable lattice spacing dependence in the RBC domain wall fermion results indicating an upward trend in the continuum limit. Indeed before comparing results too closely, discretization effects must be removed. Table 1 lists

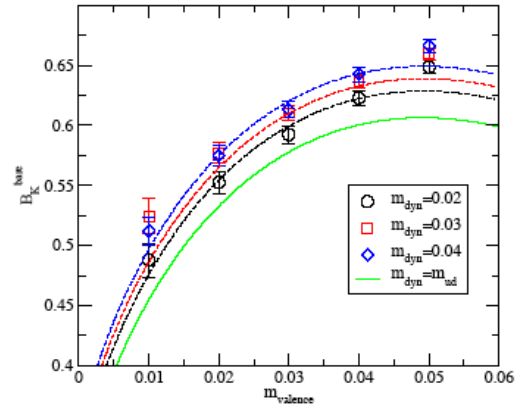


Figure 11. Bare B_K vs. mass of valence quark computed on the $n_f = 2$ RBC lattices with domain wall fermions [47]. The physical result is obtained by interpolating to $am_{\text{val}} = 0.022$, corresponding to $m_s/2$. The data at $am_{\text{val}} = 0.01$ are discarded due to poor plateaux. Curves are from a fit to NLO PQ χ PT.

several results for B_K in the continuum limit (the DWF extrapolations both based on 2 lattice spacings). The disagreement between results is not too severe. A clearer picture may emerge as studies with improved staggered fermions [41,42] and overlap fermions [43] are pursued further.

More importantly for phenomenology, unquenched calculations for B_K are underway. Furthest along are the $n_f = 2$ domain wall fermion results [47]. Fig. 11 shows B_K as a function of valence quark mass; different sea quark masses are denoted by different symbols. At $am_{\text{val}} = 0.022$, where physical results are quoted, the data tend to decrease with the sea quark mass. They quote $B_K(\overline{MS}, 2 \text{ GeV}) = 0.509(18)$ using only degenerate mass mesons. If they use nondegenerate valence quarks, and extrapolate the light mass to the physical limit they find 0.496(17). A correlated fit resolves the difference between these, hinting that SU(3) breaking effects are becoming measurable. These results are significantly lower than the quenched results in Table 1, and effect larger than anticipated from Q χ PT [48]. The authors caution that simulations at finer lat-

tice spacing (as well as finite volume and lighter sea quark mass) are necessary to estimate all the systematic effects.

Unquenched data for B_K using improved Wilson fermions recently appeared [49]. The authors note that the errors are too big and the sea quark masses are too large for reliable extrapolation to the physical masses. However, they argue that their data indicate B_K should decrease in the limit of physical sea quark masses based on the observation of the partially quenched points (shown in Fig. 12) decreasing at any given value of m_{val} as the sea quark mass is decreased. Given that the lightest $m_{\text{sea}} \approx 1.4m_s$, I do not think the trend seen in Fig. 12 necessarily continues all the way to and through the chiral regime.

B_K is also being calculated on the $n_f = 2 + 1$ MILC configurations; preliminary bare results were presented here [42]. There is some concern that, after the renormalization constant is computed, this result will agree with the quenched JLQCD result [44] and consequently disagree sharply with the $n_f = 2$ RBC result [47]. Such comparison, however, is unjustified until the matching is done for [42] and systematic uncertainties are better estimated.

6. OUTLOOK

Now that unquenched lattice calculations are able to push to lighter quark masses, well inside the chiral regime in the case of staggered fermions, predictions for phenomenology are becoming more accurate. Once the ambiguities and uncontrolled errors of the quenching are behind us, we can concentrate on more reliable estimates of the controllable uncertainties.

Already unquenched lattice results for many important quantities are being obtained. Fig. 1 shows the comparison for many quantities which are well known experimentally. Table 2 summarizes the results presented here. The precision of the lattice calculations for $|V_{us}|$ and $|V_{ub}|$ are comparable in precision to the Review of Particle Physics numbers [26], and the heavy-light decay constants are predictions. I believe the systematic uncertainties in calculations of f_B and B_K will soon reach the level where they too can be

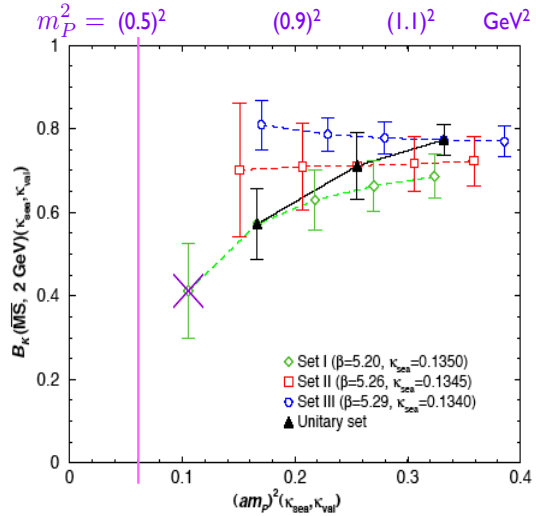


Figure 12. B_K vs. mass of valence pseudoscalar meson computed on the $n_f = 2$ UKQCD lattices with improved Wilson fermions [49]. Increasing κ implies decreasing m_{sea} . The lightest point is thrown out. The vertical line denotes the physical m_K^2 .

entered in the table. These latter 2 are especially crucial to constraints on the CKM parameters $\bar{\rho}$ and $\bar{\eta}$.

ACKNOWLEDGMENTS

This talk profited from correspondence and conversation with A. Ali Khan, I. Allison, D. Bećirević, C. Bernard, C. Davies, C. Dawson, T. DeGrand, K. Foley, E. Gamiz, S. Gottlieb, A. Gray, E. Gulez, S. Hashimoto, Y. Kayaba, A. Kronfeld, L. Lellouch, C.-J.D. Lin, V. Lubicz, P. Mackenzie, J. Noaki, M. Okamoto, F. Palombi, C. Pena, O. Pène, S. Sharpe, I. Shipsey, J. Shigemitsu, J. Simone, A.S.B. Tariq, and N. Yamada. The author is supported by DOE grant DE-FG02-00ER41132.

REFERENCES

1. V. Lubicz, arXiv:hep-lat/0410051.
2. I. Shipsey, arXiv:hep-lat/0411009.

Table 2

Summary of unquenched results for phenomenology. (See [11,18] for B_B factors.) On the left side, errors are quoted (stat)(sys), on the right, (expt)(latt). An asterisk indicates a result is preliminary.

quantity	Lattice 2004 result	Ref.	quantity	Lattice 2004 result	Ref.	RPP 2004 [26]
f_π	129.5(0.9)(3.5) MeV	[23]	$ V_{us} $	0.2219(26)	[23]	0.2200(26)
f_K	156.6(1.0)(3.6) MeV	[23]	$ V_{ub} $	$3.3(7)(4) 10^{-3}$	[23]	$3.7(5) 10^{-3}$
f_D	$224^{(+10)}_{(-14)}(21)$ MeV	[13]*	$ V_{cd} $	0.239(20)(26)	[34]	0.224(12)
f_{D_s}	$263^{(+5)}_{(-9)}(24)$ MeV	[13]*	$ V_{cs} $	0.97(2)(10)	[34]	0.996(13)
f_{B_s}	260(7)(28) MeV	[7]	$ V_{cb} $	0.038(6)(1)	[28]*[33]*	0.0413(15)

3. C. T. H. Davies *et al.* Phys. Rev. Lett. **92**, 022001 (2004).
4. C. W. Bernard *et al.*, Phys. Rev. D **64**, 054506 (2001).
5. N. Ishizuka, Nucl. Phys. Proc. Suppl. **119**, 84 (2003).
6. R. Sommer, arXiv:hep-ph/0309320.
7. M. Wingate *et al.*, Phys. Rev. Lett. **92**, 162001 (2004).
8. C. Bernard *et al.*, Phys. Rev. D **66**, 094501 (2002).
9. A. Ali Khan *et al.*, Phys. Rev. D **64**, 034505 (2001).
10. A. Ali Khan *et al.*, Phys. Rev. D **64**, 054504 (2001).
11. S. Aoki *et al.*, Phys. Rev. Lett. **91**, 212001 (2003).
12. A. X. El-Khadra, A. S. Kronfeld and P. B. Mackenzie, Phys. Rev. D **55**, 3933 (1997).
13. J. Simone *et al.*, arXiv:hep-lat/0410030.
14. A. X. El-Khadra *et al.*, Phys. Rev. D **58**, 014506 (1998).
15. C. Aubin and C. Bernard, arXiv:hep-lat/0409027.
16. M. Wingate *et al.*, Nucl. Phys. Proc. Suppl. **129**, 325 (2004).
17. A. Gray *et al.*, arXiv:hep-lat/0409040.
18. N. Yamada *et al.*, Nucl. Phys. Proc. Suppl. **106**, 397 (2002).
19. A. S. Kronfeld and S. M. Ryan, Phys. Lett. B **543**, 59 (2002).
20. D. Arndt and C.J.D. Lin, Phys. Rev. D **70**, 014503 (2004).
21. A. Abada *et al.*, Phys. Rev. D **66**, 074504 (2002).
22. A. Abada *et al.*, JHEP **0402**, 016 (2004).
23. C. Aubin *et al.* arXiv:hep-lat/0407028.
24. C. Aubin *et al.* arXiv:hep-lat/0409041.
25. W. J. Marciano, arXiv:hep-ph/0402299.
26. S. Eidelman *et al.*, Phys.Lett. B**592** (2004) 1.
27. D. Bećirević *et al.*, JHEP **0204**, 025 (2002).
28. J. Shigemitsu *et al.*, arXiv:hep-lat/0408019.
29. D. Bećirević and A. B. Kaidalov, Phys. Lett. B **478**, 417 (2000).
30. S. B. Athar *et al.*, Phys. Rev. D **68**, 072003 (2003).
31. K. M. Foley and G. P. Lepage, Nucl. Phys. Proc. Suppl. **119**, 635 (2003).
32. K. M. Foley *et al.*, this conference.
33. M. Okamoto *et al.*, arXiv:hep-lat/0409116.
34. C. Aubin *et al.*, arXiv:hep-ph/0408306.
35. D. Bećirević *et al.*, arXiv:hep-ph/0403217.
36. S. Hashimoto *et al.*, Phys. Rev. D **61**, 014502 (2000).
37. R. Gupta, arXiv:hep-lat/0303010.
38. D. Bećirević *et al.*, arXiv:hep-lat/0407004.
39. P. Dimopoulos *et al.*, arXiv:hep-lat/0409026.
40. J. Noaki, arXiv:hep-lat/0410026.
41. W. Lee *et al.*, arXiv:hep-lat/0409047.
42. E. Gamiz *et al.*, arXiv:hep-lat/0409049.
43. L. Lellouch, this conference.
44. S. Aoki *et al.*, Phys. Rev. Lett. **80**, 5271 (1998).
45. T. DeGrand, Phys. Rev. D **69**, 014504 (2004).
46. A. Ali Khan *et al.*, Phys. Rev. D **64**, 114506 (2001).
47. C. Dawson, arXiv:hep-lat/0410044.
48. S. R. Sharpe, Nucl. Phys. Proc. Suppl. **53**, 181 (1997) [arXiv:hep-lat/9609029].
49. J. M. Flynn, F. Mescia, and A.S.B. Tariq, arXiv:hep-lat/0406013.